Title

Overcoming insecticide resistance through computational inhibitor design

Authors

Galen J. Correy,[1] Daniel Zaidman,[2] Silvia Carvalho,[3] Peter D. Mabbitt,[1] Peter J. James,[4] Andrew C. Kotze,[5] Nir London,[2]* Colin J. Jackson[1]*

[1] Research School of Chemistry, Australian National University, Canberra, ACT, 2601, Australia

[2] Dept. of Organic Chemistry, The Weizmann Institute of Science, Rehovot, 76100, Israel

[3] Maurice and Vivienne Wohl Institute for Drug Discovery, Nancy and Stephen Grand Israel National Center for Personalized Medicine, The Weizmann Institute of Science, Rehovot, 76100, Israel

[4] Queensland Alliance for Agriculture and Food Innovation, The University of Queensland, Queensland, 4072, Australia

[5] CSIRO Agriculture and Food, St Lucia, Queensland, 4067, Australia

Abstract

Insecticides allow control of agricultural pests and disease vectors and are vital for global food security and health. The evolution of resistance to insecticides, such as organophosphates (OPs), is a serious and growing concern. OP resistance often involves sequestration or hydrolysis of OPs by carboxylesterases. Inhibiting carboxylesterases could therefore restore the effectiveness of OPs for which resistance has evolved. Here, we use covalent computational design to produce nano/pico-molar boronic acid inhibitors of the carboxylesterase αE7 from the agricultural pest *Lucilia cuprina*, as well as a common Gly137Asp αE7 mutant that confers OP resistance. These inhibitors, with no intrinsic apparent toxicity, act synergistically with the OPs diazinon and malathion to reduce the amount of OP required to kill *L. cuprina* by up to 16-fold, and abolish resistance. These compounds represent a solution to insecticide resistance as well as to environmental concerns regarding OPs, allowing significant reduction of use without compromising efficacy.

Introduction

As the world population increases, agricultural productivity is essential for sustaining food security. This has been facilitated through the use of pesticides and insecticides for protecting crops and livestock[1]. In terms of global health, insecticides are the first line of defense against many infectious diseases; they are especially important in developing countries, where insect vectors are responsible for nearly 20% of all infectious diseases[2]. Insecticide infused nets and residual spraying of dwellings are amongst the most effective means to control the spread of these diseases[3]. However, the widespread use of insecticides has effectively selected for insects that are resistant to the toxic effects[4]. Insecticide resistance is widespread and is an urgent global problem. Since the 1940s the number of insect species with reported insecticide resistance has been rapidly increasing, and recently passed 580 species[5]. Such resistance renders insecticides ineffective, and leads to increased usage with significant consequences to non-target species and harm to agricultural workers[5,6].

Organophosphates (OPs) and carbamates are two of the most widely used classes of insecticides[7]. They inhibit acetylcholinesterase (AChE) at cholinergic neuromuscular junctions, by phosphorylating/carbamylating the active site serine nucleophile[8]. This leads to interminable nerve signal transduction and death[9]. Resistance to OPs and carbamates has been documented in many insect species[4], with the most common mechanism of resistance involving carboxylesterases (CBEs)[10]. Resistance-associated CBEs are either overexpressed to sequester insecticides[11], or mutated to gain a new hydrolase function[12,13]; both mechanisms allow CBEs to intercept insecticides before they reach their target, AChE. The sheep blowfly *Lucilia cuprina* has become a model system for the study of insecticide resistance: resistance was first documented in 1966[14], which was found to predominantly result from a Gly137Asp mutation in the gene encoding the αE7 CBE[15]. This resistance allele now dominates contemporary blowfly populations[16], and the equivalent mutation has been observed in a range of other OP-resistant fly species[13,17]. Recent work has shown that the wild type (WT) αE7 protein also has some protective effect against OPs through its ability to sequester the pesticides[18].

Recent attempts to overcome insecticide resistance have focused on the development of new insecticides with novel modes of action[19,20]. Although many of these new targets show promise, there are a finite number of biochemical targets and new targets are not immune from the problems of target site insensitivity and metabolic resistance. Synergists have been used in the past, to enhance the efficacy of insecticides by inhibition of enzymes involved in insecticide detoxification; a prominent example of one of the few established insecticide

synergists is piperonyl butoxide, a non-specific inhibitor of cytochrome P450s[21], which is used to enhance the activity of carbamates and pyrethroids[22]. The idea of synergists can be taken further, to specifically target enzymes that have evolved to confer metabolic resistance, thereby restoring the efficacy of the insecticide to pre-resistance levels. Thus, CBEs such as αE7, being a relatively well-understood detoxification system, are ideal targets for the design of inhibitors to abolish insecticide resistance (**Fig. 1**).

Here, we report the computational design of potent and selective covalent inhibitors of αE7 using DOCKovalent. DOCKovalent is a general method for screening large virtual libraries for the discovery of specific covalent inhibitors[23,24]. An initial screen of 23,000 boronic acids against the crystal structure of αE7[25] identified picomolar-to-nanomolar inhibitors of WT αE7. Improving our understanding of the structure-activity relationships underlying the interaction enabled inhibitor optimization, resulting in a potent and selective inhibitor of both WT and the resistance associated Gly137Asp enzymes. Bioassays of blowfly survival confirmed that the optimized inhibitor synergized with OP insecticides and abolished resistance. These compounds show no significant intrinsic toxicity to flies or human cell lines, as well as very high selectivity against a panel of 26 human serine/threonine proteases. They can overcome resistance to cheap and available insecticides, while lowering the overall amount of insecticide required by more than an order of magnitude. Such synergists could have major economic and environmental benefits. The general approach demonstrated in this work should be applicable to additional CBEs as a route to fight insecticide resistance.

Results

Virtual screen of boronic acids against *Lc*αE7

*Lc*αE7 catalyzes the hydrolysis of fatty acid substrates via the canonical serine hydrolase mechanism[18,25]. Boronic acids are known to form reversible covalent adducts to the catalytic serine of serine hydrolases, which mimic the geometry of the transition state for carboxylester hydrolysis and therefore bind with high affinity[26]. We used DOCKovalent, an algorithm for screening covalent inhibitors, to screen a library of 23,000 boronic acids against the crystal structure of *Lc*αE7 (PDB code 4FNG). Each boronic acid was modelled as a tetrahedral species covalently attached to the catalytic serine (Ser218) (**Supplementary Fig. 1**). After applying the covalent docking protocol, the top 2% of the ranked library was manually examined, and five compounds ranked between 8 and 478 (**Fig. 2**) were selected for testing on the basis of docking score, ligand efficiency, molecular diversity, correct representation of the molecule and internal strain (ligand internal energy is not part of the scoring function). Additionally, we selected poses in which either hydroxyl of the boronic acid was predicted to occupy the oxyanion hole of the enzyme (**Supplementary Fig. 1**).

Selective inhibitors of WT *Lc*αE7

The potency of the boronic acids was determined by enzymatic assays of recombinant *Lc*αE7 with the model carboxylester substrate 4-nitrophenol butyrate. All five boronic acids exhibited K_i values lower than 12 nM (**Table 1**), with the most potent compound (**3**) exhibiting a K_i value of 250 pM. While the five compounds are diverse, they all share a phenylboronic acid (PBA) sub-structure, which inhibits *Lc*αE7 with a K_i value approximately 2-3 orders of magnitude lower that the designed compounds (210 nM). Compared to the nanomolar inhibition of *Lc*αE7, PBA exhibits micromolar[27] to millimolar[28] inhibition of other serine hydrolases.

To characterize the selectivity of boronic acids **1** to **5**, we assayed them against AChE, the target of OP and carbamate insecticides. None of the five compounds showed significant inhibition of AChE when tested up to their solubility limits (**Table 1**), with the most potent compound **3** displaying $>10^6$ fold selectivity for *Lc*αE7 over AChE. We further tested compound **3** against a panel of 26 human serine or threonine proteases (**Supplementary Table 1** and **2**). At a 100 μM compound concentration (10^4-fold higher than the K_i for *Lc*αE7), only 3 of the 26 proteases were inhibited by more than 50% and even those had residual activity of at least 30%. We further assessed the toxicity of the hits against two human cell lines. None of the five compounds were toxic to MDA-MB-231 cells up to 100

μM, and only compounds **2** and **5** showed limited toxicity against HB-2 cells at relatively high concentrations (IC_{50} = 20.5 μM and 77.8 μM respectively; **Table 1** and **Supplementary Fig. 2**). Overall, these data establish that the compounds are highly selective to their target with minimal off-target effects.

Crystallography validates docking pose predictions

We solved the co-crystal structures of compounds **1** to **5** with *Lc*αE7 to assess the binding poses predicted by DOCKovalent (**Fig. 2, Supplementary Table 3**). Difference electron density maps show the boronic acid compounds covalently bound to the catalytic serine (**Fig. 2**). The fit of the boronic acids to the binding pocket varies with substitution pattern; the 3,5-disubstitution of compound **3** is highly complementary while the 3,4-disubstituted arrangement of the remaining compounds results in sub-optimal arrangement depending on relative substituent size (**Fig. 2**). (For detailed descriptions of the boronic acid co-crystals structures see **Supplementary Fig. 3-6**.)

Comparison between the various co-crystal structures and the docked poses largely validates the DOCKovalent predictions (**Fig. 2**). Compounds **3** and **5** were accurately predicted with root mean square deviation (RMSD) of only 1.11 Å and 1.61 Å respectively. This orientation of the proximal ring was reproduced in all structures. For compound **1,** docking predicted a flipped orientation with respect to the bromine substituent (RMSD 2.04 Å). For compound **2** the prediction of the distal ring was not accurate (RMSD 3.01 Å). This may be due to some inherent flexibility. A lack of stabilization is reflected by 55% higher crystallographic B-factors for the distal ring compared to the proximal ring. Finally, the naphthalene ring of **4** was flipped (RMSD 2.02 Å) which required a change in conformation of Met308 (**Supplementary Fig. 3**).

Potent inhibitors of Gly137Asp *Lc*αE7

The two most common CBE-mediated insecticide resistance mechanisms involve increased protein expression, or mutation to gain new catalytic (OP-hydrolase) functions. The Gly137Asp mutation is located in the oxyanion hole and positions a new general base in the active site to catalyze dephosphorylation of the catalytic serine[15,29]. Thus, compounds that inhibit WT *Lc*αE7 as well as this common resistance associated Gly137Asp variant would increase the efficacy of OPs by targeting both detoxification routes. Encouraged by the activity of the boronic acids **1** to **5**, we tested the compounds against the Gly137Asp variant of *Lc*αE7 (**Table 1**). The most potent compound was **2**, exhibiting a K_i of 29 nM. The decreased affinity of all compounds for Gly137Asp *Lc*αE7 suggests that the Asp137 side

chain is impeding binding. This is consistent with the higher affinity of both OP and carboxylester substrates for WT *Lc*αE7 relative to Gly137Asp *Lc*αE7[29].

Optimization of Gly137Asp *Lc*αE7 inhibition

To improve Gly137Asp inhibition while maintaining good WT potency, we focused on elaborating compound **3**, the most potent WT inhibitor. We tested 12 analogues of 3-bromo phenylboronic acid with the 3,5-disubstitution pattern of compound **3** (**Fig. 3**) and determined their K_i values for WT and Gly137Asp *Lc*αE7 (Table 2). While we did not find a more potent inhibitor of WT *Lc*αE7, six of the 12 analogs exhibited picomolar K_i values (**Table 2**). This establishes a stable structure-activity relationship between the 3,5-disubstituted phenylboronic acid and high affinity WT *Lc*αE7 binding. Importantly, analogs **3.9** and **3.10**, which possess the 3,5-disubstitution pattern and flexible linkers, exhibited a 4.4- and 6.1-fold improvement in inhibition of Gly137Asp *Lc*αE7 respectively, compared to compound **3**. Both optimized compounds **3.9** and **3.10** do not exhibit any cellular toxicity up to 100 μM (**Supplementary Fig. 2**), nor potent inhibition across the panel of 26 human proteases (**Supplementary Table 1**).

To investigate the binding of the most potent inhibitor of Gly137Asp *Lc*αE7, compound **3.10**, we solved the co-crystal structure to 1.75 Å (**Supplementary Table 3**). mF_O-DF_C difference density shows the boronic acid covalently bound to the catalytic serine (**Fig. 3**). The orientation of **3.10** is conserved compared to **3**, with the 3-bromo substituent located in the larger binding pocket subsite, and the 5-methoxy-phenol substituent orientated toward the binding pocket funnel (**Fig. 3**). (For a description of conformational change within the active site of Gly137Asp αE7 upon **3.10** binding see **Supplementary Fig. 7**.)

***Lc*αE7 inhibitors synergistically enhance insecticides against blowfly larvae**

We then investigated whether the boronic acid compounds could act as synergists to restore the effectiveness of OP insecticides. Compounds were initially tested against an OP-susceptible laboratory strain of *L. cuprina* (**Fig. 4** and **Supplementary Table 4**). The efficacy of the inhibitors was determined by treating larvae with diazinon over a range of concentrations in the presence or absence of the boronic acid compounds at constant concentration, and comparing pupation. Compounds **2**, **3**, **3.9**, **3.10** and **5** were selected for testing based on high potency against WT and/or Gly137Asp *Lc*αE7, and their structural diversity. In assays of the susceptible strain with diazinon, synergism was observed for compounds **3**, **3.9** and **3.10**. Compound **3.10** was the most potent, decreasing the amount of diazinon required to achieve a 50% reduction in pupation (EC_{50} value) 5.7-fold compared to a diazinon only control (**Fig. 4**). The observed differences in the levels of synergism for

compounds **3**, **3.9** and **3.10** could be related to differences in the bioavailability of the compounds, since their *in vitro* potency is very similar.

To confirm that the observed synergism was due to *Lc*αE7 inhibition, and not due to toxic side-effects of the boronic acid compounds, we also tested the compounds in the absence of diazinon (**Supplementary Fig. 8**). There was no significant difference between the fly pupation rates in the presence or absence of the boronic acids compounds. This is consistent with *in vitro* tests showing that these compounds have low (mM) affinity for AChE, our cellular toxicity data, and the known low toxicity of boronic acids[30].

Having demonstrated synergism between the boronic acids and an OP insecticide, we tested the compounds against a field strain of *L. cuprina* resistant to diazinon. Diazinon resistance is typically associated with the Gly137Asp mutation/resistance allele. We determined the genotype of the field strain used in the bioassays and found that, although the laboratory strain carried only WT susceptible alleles (Gly137), the field strain carried both susceptible (Gly137) and resistance (Asp137) alleles (**Supplementary Fig. 9**). This is consistent with previous results showing that duplications of the chromosomal region containing αE7 have occurred, meaning that resistant strains now carry copies of both WT and Gly137Asp *Lc*αE7[31]. Resistance can be quantified by the increase in the insecticide EC_{50}. The diazinon EC_{50} for the (resistant) field strain was 2.9-fold higher compared to the (susceptible) laboratory strain (**Fig. 4**). All the boronic acids tested were observed to increase the efficacy of diazinon, reducing the EC_{50} values. The most effective compound (**3.10**) reduced the of EC_{50} with the susceptible strain 12-fold. Compound **3.10** therefore not only abolished the 2.9-fold greater OP resistance in the field strain of *L. cuprina* (as measured by EC_{50}), but actually made it 4-fold more sensitive to diazinon, when compared to the susceptible strain (when treated with only diazinon). We observed similar synergism for both the laboratory and resistant strains when the concentration of boronic acid used in the bioassays was decreased from 1 mg/ml to 0.25 or 0.06 mg/ml (**Supplementary Fig. 10**).

Based on the *in vitro* enzyme inhibition profile (**Table 1**), the higher level of diazinon synergism in the field strain with compound **3** versus compound **2** is surprising. However, this discrepancy is consistent with the observation that contemporary resistant strains contain both WT and Gly137Asp alleles *Lc*αE7[32]. (This is also consistent with our DNA sequencing data; **Supplementary Fig. 9**.) Specifically, a compound, such as **3.10** that effectively inhibits both *Lc*αE7 variants would be the best synergist against a resistant strain. The synergism exhibited by compound **3.10** is therefore a function of the optimized Gly137Asp *Lc*αE7 inhibition and retention of WT *Lc*αE7 inhibition. This highlights the

importance of both sequestration (*via* WT) and catalytic detoxification (*via* Gly137Asp) by *Lc*αE7 in OP resistance.

We also tested the effects of compounds **3**, **3.9** and **3.10** on the sensitivity of the laboratory strain to the OP insecticide malathion. Sensitivity to malathion and diazinon is qualitatively different; WT *Lc*αE7 confers a low level of resistance to diazinon via high affinity binding and slow hydrolysis, however WT *Lc*αE7 displays significant malathion hydrolysis activity[13]. This difference is evident in the similar EC_{50} values for the laboratory *L. cuprina* strain treated with malathion compared to the field (resistant) strain treated with diazinon (**Fig. 4**). Synergism with malathion was observed for all the boronic acid compounds tested. Compound **3.10** was the most effective, reducing the EC_{50} 16-fold compared to a malathion only control (**Fig. 4** and **Supplementary Table 4**).

Discussion

The design of potent and selective enzyme inhibitors is a central challenge in chemical biology[33]. Despite the prominence and investment in high-throughput screening technologies, virtual compound screens provides an inexpensive and rapid alternative[34]. Here, we implemented a virtual screen of 23,000 boronic acid compounds to identify inhibitors of *Lc*αE7. The 100% hit rate from the initial screen, with all compounds exhibiting K_i values lower than 12 nM, is surprisingly high, even when compared to previous covalent virtual screens that exhibited high hit rates against diverse enzyme targets[23]. This can be partly attributed to the privileged status of PBA as an inhibitor of *Lc*αE7. The K_i of PBA for *Lc*αE7 is 10- to 1000-fold better compared to other serine hydrolases[27,28]. Although 74% of the screening library contained this substructure, the docking still enriched it in the top hits (86% of the top 500) and the specific suggested modifications on the basic scaffold afforded up to 3 orders-of-magnitude improvement. Therefore, although virtual screening methods will benefit from improvements to sampling and scoring, reflected by the fact that there was no correlation between docking rank and inhibitor potency for the compounds from the initial screen (**Table 1**), application of the DOCKovalent method allowed the rapid identification and optimization of potent inhibitors of *Lc*αE7, with the initial testing of only five compounds.

Insecticides remain the primary measure for control of agricultural pests, such as the sheep blowfly, as well as disease vectors, such as mosquitoes. The constant evolution of pesticide resistance in almost all species makes the development of new approaches to prevent or abolish resistance of great importance. While there is hope for the development of new pesticides, there are a finite number of biochemical targets and the use of synergists to knock out the resistance mechanisms and restore the effectiveness of OP insecticides is a viable alternative strategy. In this work, we have targeted CBEs, which have been associated with over 50 cases of pesticide resistance over the last 50 years[10]. The observation that a Gly>Asp mutation at an equivalent position to 137 in other insect pests[13,17], and the relatively high sequence conservation of metabolic insect CBEs[10], suggests that the synergists such as those developed in this work could have broad spectrum activity against a range of insect species. An added benefit of boronic acid synergists is the potential protection from the evolution of resistance. Since boronic acids are transition state analogues for the phosphorylation of the catalytic serine by OP insecticides, mutations that hinder boronic acid binding will also likely disrupt OP sequestration and/or hydrolysis.

A major requirement for such synergists to be practical is a benign safety and environmental profile. The main concern in terms of toxicity is selectivity against AChE. While the overall structure of *Lc*αE7 resembles that of human AChE (PDB 4PQE; 1.05Å RMSD over 309 residues), the enzymes are quite different in the region of the active site[25], which results in the >10^6 fold selectivity of compound **3** for *Lc*αE7 (**Table 1**). As a result of the conformational differences in the active sites, the bromo- substituent, which is highly complementary to the *Lc*αE7 active site, is sterically occluded from the active site of AChE due to a clash with Phe295 in (**Supplementary Fig. 11**). Moreover, we demonstrated that these compounds do not significantly inhibit other non-target proteins such as human serine and threonine proteases, nor are they generally toxic to cells. While these are not comprehensive proof, they are consistent with other literature suggesting that boronic acids are relatively benign[30]. Organophosphate insecticides are used worldwide; an estimated 9 million kilograms are applied annually in the United States alone[7]. Our *in vivo* results indicate that administration in combination with these or similar synergists may reduce OP use by more than an order of magnitude. Such a reduction, without compromising efficacy, could have enormous health, environmental and economic consequences.

The potent and selective *Lc*αE7 inhibitors reported in this work represent a milestone in the use of virtual screening for inhibitor discovery in the context of combating pesticide resistance. We identified high affinity boronic acid inhibitors of a key resistance enzyme, and developed our understanding of the general structure-activity relationships that underlie the effectiveness of boronic acids with serine hydrolases, facilitating inhibitor optimization. The demonstration that the compounds effectively abolished OP insecticide resistance in *L. cuprina*, without significant toxicity on their own or significant inhibition of human enzymes, establishes the viability of this synergist-focused approach to combat pesticide resistance and restore the effectiveness of existing pesticide classes. The substantial increase in insecticide efficacy would allow more sustainable pesticide usage and reduce off-target environmental and health-related pesticide effects.

Acknowledgements

We thank Paul Carr for assistance with X-ray crystallography and the Australian Synchrotron for beam time. This research was supported by the Australian Research Council (Future Fellowship to C. J. J.; FT140101059), Australian Science and Industry Endowment Fund (C. J. J. and P. D. M.; PF14-099), an Australian Postgraduate Award (G. J. C.) and the ISRAEL SCIENCE FOUNDATION (grant No. 1097/16) to N.L.

Author contributions

N.L. and C.J.J. directed the project. N.L. and D.Z. performed covalent docking and computational analysis. G.J.C. determined the crystal structures and performed biochemical characterization. P.J.J. and A.C.K. performed blowfly assays. S.C. performed cellular toxicity assays. G.J.C., P.D.M., N.L. and C.J.J. wrote the paper. All authors contributed to the manuscript in its final form.

Competing financial interests

G.J.C., N.L. and C.J.J., are inventors on a US patent application (62/443,825) for the described synergists.

Materials & Correspondence

Correspondence and requests for materials should be addressed to N.L. or C.J.J.

Accession codes.

All crystal structures reported here were deposited in the PDB under accession codes 5TYP, 5TYO, 5TYN, 5TYL, 5TYK, 5TYM and 5TYJ.

References

1. Cooper, J. & Dobson, H. The benefits of pesticides to mankind and the environment. *Crop Prot.* **26,** 1337–1348 (2007).
2. World Health Organization. *Integrated vector management: Strategic framework for the Eastern Mediterranean region 2004-2010*. (The WHO Regional Office for the Eastern Mediterranean, 2004).
3. World Health Organization. *Pesticides and their application for the control of vectors and pests of public health importance*. (World Health Organization, 2006).
4. Whalon, M. E., Mota-Sanchez, D. & Hollingworth, R. M. *Global pesticide resistance in arthropods*. (Cabi International, 2008).
5. Sparks, T. C. & Nauen, R. IRAC: Mode of action classification and insecticide resistance management. *Pestic. Biochem. Physiol.* **121,** 122–128 (2015).
6. Eddleston, M. *et al.* Pesticide poisoning in the developing world - A minimum pesticides list. *Lancet* **360,** 1163–1167 (2002).
7. Atwood, D. & Paisley-Jones, C. Pesticides industry sales and usage 2008-2012 Market estimates. *U.S. Environ. Prot. Agency* (2017).
8. Fukuto, T. R. Mechanism of action of organophosphorus and carbamate onsecticides. *Environ. Health Perspect.* **87,** 245–254 (1990).
9. Tafuri, J. & Roberts, J. Organophosphate poisoning. *Ann. Emerg. Med.* **16,** 193–202 (1987).
10. Oakeshott, J. G., Claudianos, C., Campbell, P. M., Newcomb, R. D. & Russell, R. J. in *Comprehensive Molecular Insect Science - Pharmacology* (eds. Gilbert, L. I. & Gill, S. S.) 309–381 (Elsevier B.V., 2005).
11. Devonshire, A. L. & Field, L. M. Gene amplivication and insecticide resistance. *Annu. Rev. Entomol.* (1991).
12. Newcomb, R. D., Gleeson, D. M., Yong, C. G., Russell, R. J. & Oakeshott, J. G. Multiple mutations and gene duplications conferring organophosphorus insecticide resistance have been selected at the Rop-1 locus of the sheep blowfly, Lucilia cuprina. *J. Mol. Evol.* **60,** 207–20 (2005).
13. Claudianos, C., Russell, R. J. & Oakeshott, J. G. The same amino acid substitution in orthologous esterases confers organophosphate resistance on the house fly and a blowfly. *Insect Biochem. Mol. Biol.* **29,** 675–686 (1999).
14. Shanahan, G. J. Development of a changed response in Lucilia cuprina (Wied.) to organophosphorus insecticides in New South Wales. *Bull. Entomol. Res.* **57,** 93 (1966).
15. Newcomb, R. D. *et al.* A single amino acid substitution converts a carboxylesterase to an organophosphorus hydrolase and confers insecticide resistance on a blowfly. *Proc.*

Natl. Acad. Sci. U. S. A. **94,** 7464–7468 (1997).

16. McKenzie, J. A. Dieldrin and diazinon resistance in populations of the Australian sheep blowfly, Lucilia cuprina, from sheep-grazing areas and rubbish tips. *Aust. J. Biol. Sci.* **37,** 367–374 (1984).
17. de Carvalho, R. A., Torres, T. T. & de Azeredo-Espin, A. M. L. A survey of mutations in the Cochliomyia hominivorax (Diptera: Calliphoridae) esterase E3 gene associated with organophosphate resistance and the molecular identification of mutant alleles. *Vet. Parasitol.* **140,** 344–351 (2006).
18. Birner-Gruenberger, R. *et al.* Functional fat body proteomics and gene targeting reveal in vivo functions of Drosophila melanogaster α-Esterase-7. *Insect Biochem. Mol. Biol.* **42,** 220–9 (2012).
19. Mao, Y.-B. *et al.* Silencing a cotton bollworm P450 monooxygenase gene by plant-mediated RNAi impairs larval tolerance of gossypol. *Nat. Biotechnol.* **25,** 1307–1313 (2007).
20. Swale, D. R. *et al.* An insecticide resistance-breaking mosquitocide targeting inward rectifier potassium channels in vectors of Zika virus and malaria. *Sci. Rep.* **6,** 36954 (2016).
21. Matthews, H. B. & Casida, J. E. Properties of housefly microsomal cytochromes in relation to sex, strain, substrate specificity, and apparent inhibition and induction by synergist and insecticide chemicals. *Life Sci.* 989–1001 (1970).
22. Metcalf, R. L. Mode of action of insecticide synergists. *Annu. Rev. Entomol.* **12,** 229–256 (1967).
23. London, N. *et al.* Covalent docking of large libraries for the discovery of chemical probes. *Nat. Chem. Biol.* **10,** 1066–72 (2014).
24. London, N. *et al.* Covalent docking predicts substrates for haloalkanoate dehalogenase superfamily phosphatases. *Biochemistry* **54,** 528–537 (2015).
25. Jackson, C. J. *et al.* Structure and function of an insect α-carboxylesterase (αEsterase7) associated with insecticide resistance. *Proc. Natl. Acad. Sci. U. S. A.* **110,** 10177–82 (2013).
26. Koehler, K. A. & Lienhard, G. E. 2-phenylethaneboronic acid, a possible transition-state analog for chymotrypsin. *Biochemistry* **10,** 2477–2483 (1971).
27. Sutton, L. D., Stout, J. S., Hosie, L., Spencer, P. S. & Quinn, D. M. Phenyl-n-butylborinic acid is a potent transition state analog inhibitor of lipolytic enzymes. *Biochem. Biophys. Res. Commun.* **134,** 386–392 (1986).
28. Kettner, C., Bone, R., Agard, D. & Bachovchin, W. Kinetic properties of the binding of. alpha.-lytic protease to peptide boronic acids. *Biochemistry* **27,** 7682–7688 (1988).
29. Mabbitt, P. D. *et al.* Conformational disorganization within the active site of a recently

evolved organophosphate hydrolase limits its catalytic efficiency. *Biochemistry* **55,** 1408–1417 (2016).

30. Hall, D. G. *Boronic acids: preparation, applications in organic synthesis and medicine*. (Wiley-VCH, 2005).
31. Smyth, K. A., Boyce, T. M., Russell, R. J. & Oakeshott, J. G. MCE activities and malathion resistances in field populations of the Australian sheep blowfly (Lucilia cuprina). *Heredity (Edinb).* **84,** 63–72 (2000).
32. Russell, R. J. *et al.* The evolution of new enzyme function: lessons from xenobiotic metabolizing bacteria versus insecticide-resistant insects. *Evol. Appl.* **4,** 225–48 (2011).
33. Probing Questions. *Nat. Chem. Biol.* **61,** 48–53 (2015).
34. Shoichet, B. K. Virtual screening of chemical libraries. *Nature* **432,** 862–865 (2004).

Online methods

Covalent virtual screen

DOCKovalent is a covalent adaptation of DOCK3.6. Given a pre-generated set of ligand conformations and a covalent attachment point, it exhaustively samples ligand poses around the covalent bond and selects the lowest energy pose using a physics-based energy function that evaluates van der Waals and electrostatics interactions as well as penalizing for ligand desolvation. For the docking performed in this work, a boronic acids library of 23,000 commercially available compounds was used.

Receptor preparation: PDB code 4FNG was used for the docking. Ser218 was deprotonated to accommodate the covalent adduct and the Oγ partial charge was adjusted to represent a bonded form. His471 was represented in its doubly protonated form.

Sampling parameters: The covalent bond length was set to 1.5 ± 0.1 Å and the two newly formed bond angles to Cβ-Oγ-B=116.0 ± 5° and Oγ-B-Ligatom=109.5 ± 5°, the boron atom was replaced by a carbon, as boron is not parameterized for some of the ligand preparation tool-chain. As the covalent attachment atom is not scored during the docking, this replacement should not influence the results.

Candidate selection: the top 500 molecules from the ranked docking list, sorted by calculated ligand efficiency (docking score divided by number of heavy atoms) were manually inspected for exclusion, based on considerations that are orthogonal to the docking scoring function such as novelty of the compounds, diversity, commercial availability, correct representation of the molecule and internal strain (ligand internal energy is not part of the scoring function). Additionally, we selected poses in which either of the boronic acid hydroxyls is predicted to occupy the oxyanion hole. Second generation compounds were selected based on the identified 3,5 phenyl-boronic acid substitution pattern from the CombiBlocks catalog.

Enzyme expression and purification

His_6-tagged proteins were expressed in BL21(DE3) *E. coli* (Invitrogen) at 26˚C for 18 hours. Cells were collected by centrifugation, resuspended in lysis buffer (300 mM NaCl, 10 mM imidazole, 50 mM HEPES pH 7.5) and lysed by sonication. Cell debris was pelleted by centrifugation and the soluble fraction was loaded onto a HisTrap-HP Ni-Sepharose column (GE Healthcare). Bound protein was eluted with lysis buffer supplemented with 300 mM imidazole. Fractions containing the eluted protein were concentrated with a 30 kDa

molecular mass cutoff centrifuge concentrator (Amicon) and loaded onto a HiLoad 26/60 Superdex-200 size-exclusion column (GE Healthcare) pre-equilibrated with 150 mM NaCl, 20 mM HEPES pH 7.5. Eluted fractions containing the monomeric protein were pooled for enzyme inhibition assays or crystallization. Protein concentration was determined by measuring the absorbance at 280 nm with an extinction coefficient calculated using the Protparam online server[1].

Enzyme inhibition assays

Inhibition of WT *Lc*αE7 and the Gly137Asp *Lc*αE7 variant was determined by a competition assay between the native-substrate analogue 4-nitrophenol butyrate (4-NPB, Sigma) and the boronic acid compounds. Initially, the Michaelis constant (K_M) with 4-NPB was measured for both enzymes to determine an appropriate concentration of substrate for use in the competition assays. Formation of the 4-nitrophenolate product of hydrolysis was monitored at 405 nm in the presence of enzyme and eight different concentrations of substrate. 4-NPB was prepared in methanol to 100 mM and serially diluted 1-in-2 to achieve concentrations from 100 mM to 0.8 mM. Enzyme stocks were prepared in 4 mg/ml bovine serum albumin (Sigma) to maintain enzyme stability. Reactions were prepared by pipetting 178 µl assay buffer (100 mM NaCl, 20 mM HEPES pH 7.5) and 2 µl substrate (final concentrations of 1000 to 8 µM) into 300 µl wells of a 96-well plate. The reaction was initiated by the addition of 20 µl enzyme (final concentration 2.5 nM for WT *Lc*αE7 and 4 nM for Gly137Asp *Lc*αE7). Product formation was monitored for four minutes at room temperature using an Epoch microplate spectrophotometer (BioTek) and the initial rates of ester hydrolysis were determined by linear regression using GraphPad Prism. The Michaelis constant was determined by fitting the initial rates to the Michaelis-Menten equation (**Supplementary Fig. 12**).

Enzyme inhibition with the boronic acid compounds was determined by assaying the initial rate of 4-NPB hydrolysis in the presence of either neat DMSO or the boronic acid compounds in DMSO. Compounds were prepared by serially diluting 1-in-3 an initial 10 mM stock to achieve concentrations from 10 mM to 6.27 nM. Reactions were prepared by pipetting 178 µl assay buffer supplemented with substrate to a final concentration equal to the K_M of the enzyme (15 µM for wild-type *Lc*αE7 and 250 µM for Gly137Asp *Lc*αE7) into wells of a 96-well plate. 2 µl neat DMSO or 2 µl serially diluted inhibitor (final concentrations of 100 µM to 62.7 pM) were added to the wells. The reaction was initiated by the addition of 20 µl enzyme (final concentration 0.5 nM for wild-type *Lc*αE7 and 10 nM for Gly137Asp *Lc*αE7). Product formation was monitored for four minutes at room temperature and the initial rates of ester hydrolysis were determined by linear regression. To determine the

concentration of boronic acid compounds required to inhibit 50% of esterase activity (IC_{50}), a four-parameter sigmoidal dose-response curve was fitted to percentage inhibition using GraphPad Prism (**Supplementary Fig. 13** and **14**). K_i values were determined using the Cheng-Prusoff equation assuming competitive inhibition[2].

AChE Selectivity

Inhibition of *Electrophorus electricus* AChE (Type V-S, Sigma) by phenylboronic acid and compounds **1**-**5** was determined using the method described by Ellman et al[3]. Initially, the K_M for AChE with the substrate acetylthiocholine was determined by monitoring thiocholine production with 5,5'-dithiobis(2-nitrobenzoic acid) (DTNB) at 412 nm. Acetylthiocholine was prepared in assay buffer (100 mM NaH_2PO_4 pH 7.4) to 10 mM and serially diluted 1-in-2 to achieve concentrations from 10 mM to 0.08 mM while AChE was prepared in 20 mM NaH_2PO_4 pH 7.0 supplemented with 4 mg/ml BSA to 0.4 nM. Reactions were prepared by pipetting 160 µl assay buffer (supplemented with DTNB to a final concentration of 300 µM) and 20 µl acetylthiocholine (1000 to 7.8 µM final concentration) into wells of a 96-well plate. The reaction was initiated by the addition of 20 µl AChE (40 pM final concentration). Product formation was monitored for six minutes at room temperature and the initial rates of thioester hydrolysis were determined by linear regression using GraphPad Prism. The Michaelis constant was determined as before (**Supplementary Fig. 12**).

AChE inhibition was determined by assaying the initial rate of acetylthiocholine hydrolysis in the presence of either neat DMSO or the boronic acid compounds in DMSO. Compounds were prepared by making serial 1-in-3 dilutions of 1 M stocks to achieve concentrations from 1 M to 627 nM. Reactions were prepared by pipetting 178 µl assay buffer supplemented with acetylthiocholine (to a final concentration of 100 µM) and DTBN (to a final concentration of 300 µM) into wells of a 96-well plate. 2 µl neat DMSO or 2 µl serially diluted inhibitor (final concentrations of 10 mM to 6.27 nM) were added to the wells. The reaction was initiated by the addition of 20 µl enzyme (final concentration 40 pM). Product formation was monitored for six minutes at room temperature and the initial rates of thioester hydrolysis were determined by linear regression. IC_{50} and K_i values were determined as described previously (**Supplementary Fig. 15**).

Protease Selectivity Panel

Compounds were tested for inhibition of a panel of 26 Ser/Thr proteases at a single point concentration of 100 µM in duplicates by NanoSyn (Santa Clara, CA). See **Supplementary Table 2** for assay conditions.

Cellular Toxicity Assays

A seven-point, two-fold dose response series, with a 100uM as the upper limit and a DMSO-only control point was generated using an Echo 550 liquid handler (Labcyte Inc.) in 384-well plates. Subsequently, the human breast cell lines MDA-MB-231 (tumorigenic) and HB2 (non-tumorigenic) were seeded (1000 cells/well) using a multi-drop Combi (Thermo Fisher Scientific) on top of the compounds. Plates were then incubated at 37ºC and 5% CO_2 for 48 hours upon which cell viability was assessed by adding CellTiter-Glo® (Promega) to the reaction. The luminescence signal was measured on a Pherastar FS multi-mode plate reader (BMG Labtech).

Crystallization and structure determination

Co-crystals of compounds **1-5** with the thermostable *Lc*αE7 variant[4,5] (*Lc*αE7-4a) (PDB code 5TYP, 5TYO, 5TYN, 5TYL and 5TLK) and compound **3.10** with Gly137Asp *Lc*αE7-4a (PDB code 5TYM) were grown using the hanging drop vapor-diffusion method. Reservoir solutions contained 100 mM sodium acetate (pH 4.6-5.1) and 15-26% PEG 2000 monomethyl ether (MME) or PEG 550 MME. Inhibitors prepared in DMSO were incubated with protein (7 mg/ml in 75 mM NaCl and 10 mM HEPES pH 7.5) to achieve a 5:1 inhibitor-to-compound stoichiometric ratio. Hanging drops were set-up with 2 µl reservoir and 1 µl protein with crystals forming overnight at 19°C. For cryoprotection, crystals were briefly immersed in a solution containing the hanging-drop reservoir solution with the PEG concentration increased to 35%, and then vitrified at 100 K in a gaseous stream of nitrogen.

Diffraction data was collected at 100 K on either the MX1 or MX2 beam line at the Australian Synchrotron using a wavelength of 0.954 Å. Data was indexed, integrated and scaled using XDS[6]. High resolution data was excluded when the correlation coefficient between random half data sets ($CC_{1/2}$)[7,8] decreased below 0.3 in the highest resolution shell. Phases were obtained by molecular replacement with the program Phaser[9] using the coordinates of apo-*Lc*αE7-4a (PDB code 5CH3) as the search model. The initial model was improved by iterative model building with COOT[10] and refinement with phenix.refine[11]. Inhibitor coordinates and restraints were generated with eLBOW[12]. Custom geometry restraints applied to the inhibitor-protein covalent bond are presented in **Supplementary Table 5**. Crystallographic statistics are summarized in **Supplementary Table 3**.

To determine if the mutations present in the thermostable *Lc*αE7-4a[4,5] influenced the orientation or mode of inhibitor binding, the surface mutations present in *Lc*αE7-4a were introduced into the WT background and the protein was tested for crystallization. Two

mutations (Lys530Glu and Asp83Ala) were sufficient to allow crystallization in the same conditions as described previously (PDB code 5TYM) (**Supplementary Fig. 5** and **16**).

***Lucilia cuprina* bioassays**

Two strains of *L. cuprina* were used: 1) a laboratory reference drug-susceptible strain, LS, derived from collections in the Australian Capital Territory over 40 years ago, with no history of exposure to insecticides; and 2) a field-collected strain, Tara, resistant to diazinon and diflubenzuron[13]. The *Lc*αE7 gene was sequenced in each of the strains. Briefly, genomic DNA was prepared from 20 adult female flies from each strain using the DNeasy Blood and Tissue kit (Qiagen). PCR was performed with primers specific to the *Lc*αE7 gene[14], and the product was cloned into a pGEM-T EASY vector (Promega). Eight clones of the susceptible strain and 10 clones of the resistant strain were sequenced using M13 forward and reverse primers.

The effect of compounds **2**, **3**, **5, 3.9** and **3.10** on the development of blowfly larvae in the presence of diazinon/malathion was assessed using a bioassay system in which larvae were allowed to develop from the first instar stage until pupation on cotton wool impregnated with diazinon/malathion over a range of concentrations, in the presence or absence of the compounds at constant concentrations[15]. Each experiment utilized 50 larvae at each diazinon/malathion concentration. Experiments were replicated three times for diazinon, and twice for malathion. The insecticidal effects were defined by measuring the pupation rate. The pupation rate dose-response data were analyzed by non-linear regression (GraphPad Prism) in order to calculate EC_{50} values (with 95% confidence intervals) representing the concentration of diazinon/malathion (alone or in combination with compounds **2**, **3**, **5, 3.9** or **3.10**) required to reduce the pupation rate to 50% of that measured in control assays. The effects of compounds **2**, **3**, **5, 3.9** and **3.10** was defined in two ways: 1) synergism ratio within each isolate = the EC_{50} for diazinon/malathion alone / EC_{50} for diazinon/malathion in combination with the compounds; and 2) resistance ratio = the EC_{50} for diazinon alone or in combination with the compounds for the Tara strain / EC_{50} for diazinon alone with the LS strain. Significant differences between EC_{50} values were assessed based on overlap of 95% confidence intervals. Compounds were also tested without diazinon or malathion at 1 mg per assay.

References

1. Gasteiger, E. *et al.* Protein identification and analysis tools on the ExPASy server. *Proteomics Protoc. Handb.* 571–607 (2005).
2. Yung-Chi, C. & Prusoff, W. H. Relationship between the inhibition constant (KI) and the concentration of inhibitor which causes 50 per cent inhibition (I50) of an enzymatic reaction. *Biochem. Pharmacol.* **22,** 3099–3108 (1973).
3. Ellman, G. L., Courtney, K. D., Andres, V. & Featherstone, R. M. A new and rapid colorimetric determination of acetylcholinesterase activity. *Biochem. Pharmacol.* **7,** 88–95 (1961).
4. Jackson, C. J. *et al.* Structure and function of an insect α-carboxylesterase (αEsterase7) associated with insecticide resistance. *Proc. Natl. Acad. Sci. U. S. A.* **110,** 10177–82 (2013).
5. Fraser, N. J. *et al.* Evolution of protein quaternary structure in response to selective pressure for increased thermostability. *J. Mol. Biol.* **428,** 2359–2371 (2015).
6. Kabsch, W. XDS. *Acta Crystallogr. Sect. D Biol. Crystallogr.* **66,** 125–132 (2010).
7. Karplus, P. A. & Diederichs, K. Linking crystallographic model and data quality. *Science* **336,** 1030–3 (2012).
8. Diederichs, K. & Karplus, P. A. Better models by discarding data? *Acta Crystallogr. D. Biol. Crystallogr.* **69,** 1215–22 (2013).
9. McCoy, A. J. *et al.* Phaser crystallographic software. *J. Appl. Crystallogr.* **40,** 658–674 (2007).
10. Emsley, P., Lohkamp, B., Scott, W. G. & Cowtan, K. Features and development of Coot. *Acta Crystallogr. Sect. D Biol. Crystallogr.* **66,** 486–501 (2010).
11. Afonine, P. A. *et al.* Towards automated crystallographic structure refinement with phenix.refine. *Acta Crystallogr. Sect. D Biol. Crystallogr.* **68,** 352–367 (2012).
12. Adams, P. D. *et al.* PHENIX: A comprehensive Python-based system for macromolecular structure solution. *Acta Crystallogr. Sect. D Biol. Crystallogr.* **66,** 213–221 (2010).
13. Levot, G. W. & Sales, N. New high level resistance to diflubenzuron detected in the Australian sheep blowfly, Lucilia cuprina (Wiedemann) (Diptera: Calliphoridae). *Gen. Appl. Entomol.* **31,** 43–46 (2002).
14. Newcomb, R. D., Campbell, P. M., Russell, R. J. & Oakeshotr, J. G. cDNA cloning, baculovirus-expression and kinetic properties of the esterase, E3, involved in organophosphate resistance in Lucilia cuprina. *Insect Biochem. Mol. Biol.* **27,** 15–25 (1997).
15. Kotze, A. C. *et al.* Histone deacetylase enzymes as drug targets for the control of the sheep blowfly, Lucilia cuprina. *Int. J. Parasitol. Drugs Drug Resist.* **5,** 201–208 (2015).

Figures

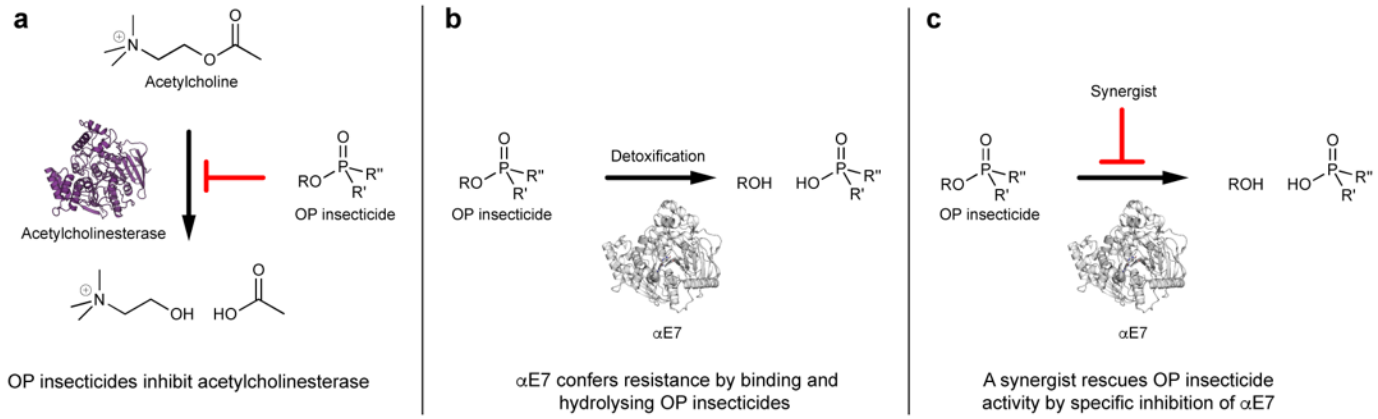

Figure 1. Overview of synergists for organophosphate insecticides. (**a**) Organophosphate insecticides inhibit acetylcholinesterase and prevent the hydrolysis of acetylcholine. (**b**) CBEs like αE7 rescue acetylcholinesterase activity by binding and hydrolyzing organophosphate insecticides. (**c**) An inhibitor that outcompetes organophosphates for binding to CBE could act as a synergist to restore insecticide activity.

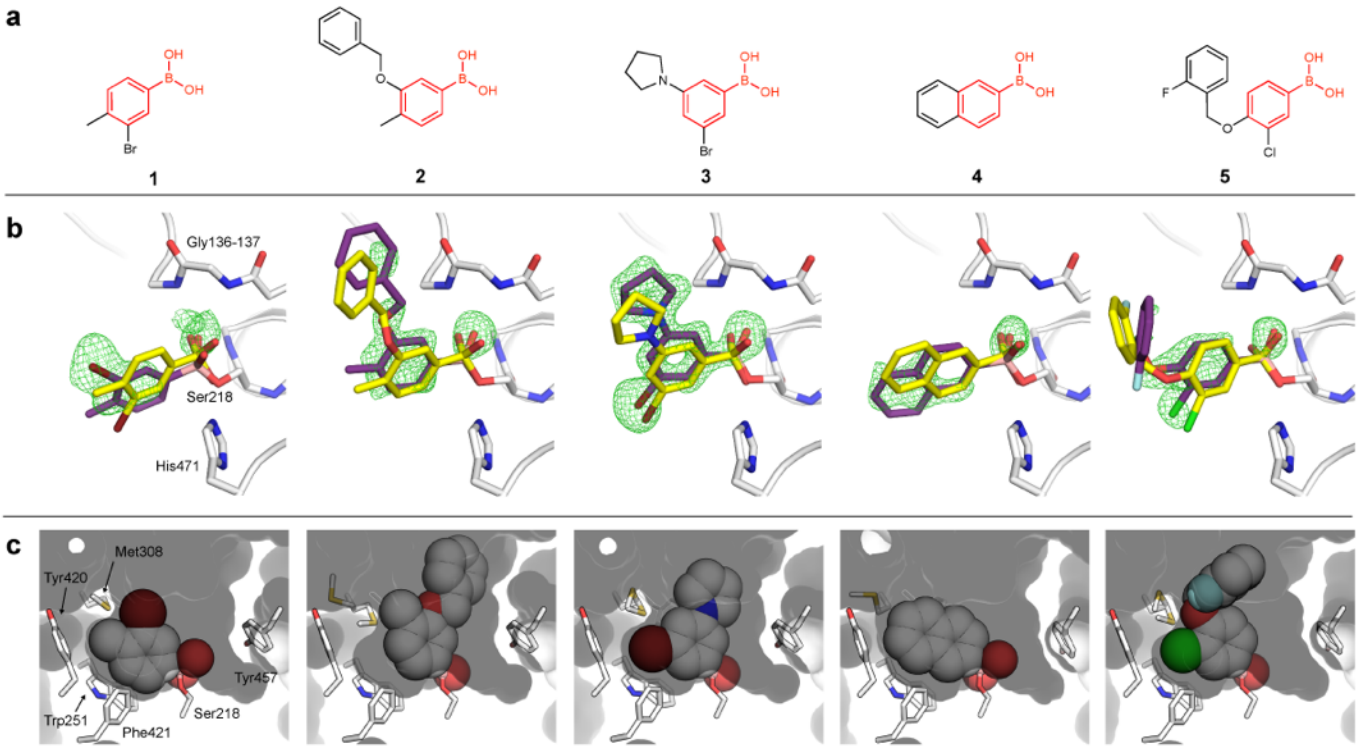

Figure 2. Covalent docking predicts potent inhibitors of *Lc*αE7. (**a**) Chemical structures of predicted *Lc*αE7 inhibitors. The conserved phenylboronic acid substructure is highlighted in red. (**b**) Compounds **1**-**5** (purple sticks) form covalent adducts with the catalytic serine of *Lc*αE7 (Ser218). The omit mF_O-DF_C difference electron density is shown (green mesh contoured at 3 σ). The docking predictions (yellow sticks) are overlaid onto the corresponding co-crystal structures. Active site residues are shown as white sticks. (**c**) Surface representation of *Lc*αE7 binding pocket with compounds **1**-**5** shown with a space-filling representation (white spheres).

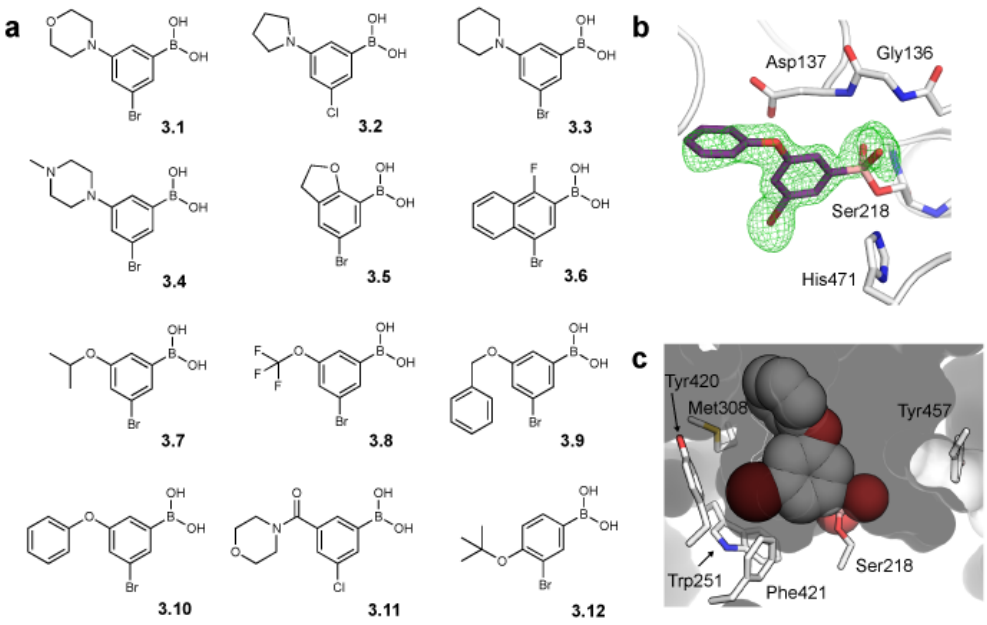

Figure 3. Second generation boronic acids are potent inhibitors of Gly137Asp *Lc*αE7. (**a**) Chemical structures of compound **3** analogues. (**b**) Co-crystal structure of compound **3.10** (purple sticks) with Gly137Asp *Lc*αE7 (PDB code 5TYM). The omit mF_O-DF_C difference electron density is shown (green mesh contoured at 3 σ). Active site residues are shown as white sticks. (**c**) Surface representation of Gly137Asp *Lc*αE7 binding pocket with compound **3.10** shown with a space-filling representation (white spheres).

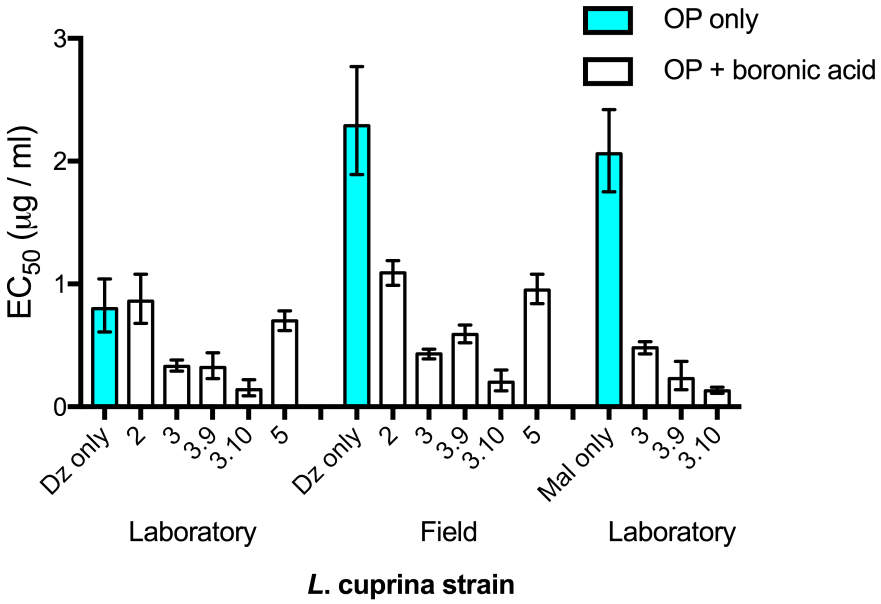

Figure 4. Boronic acid inhibitors synergize with the organophosphate insecticides diazinon and malathion. Treatment consisted of diazinon (Dz) or malathion (Mal) only, or Dz / Mal supplemented with boronic acid compound at a set concentration of 1 mg/ml. Data is presented mean ± 95% confidence interval for three (Dz) or two (Mal) replicate experiments, with each experiment utilizing 50 larvae at each Dz / Mal concentration.

Tables

Table 1. Docking rank, *in vitro* αE7 inhibition and selectivity of compounds 1-5 and phenyl boronic acid (PBA).

		K_i (nM)			Viability IC_{50} (μM)	
Comp.	DOCK rank	wildtype *Lc*αE7	Gly137Asp *Lc*αE7	*Ee* AChE[b]	MDA-MB-231[c]	HB-2[c]
PBA	-	210 (270-260)	450 (370-550)	> 10 mM	-	-
1	8	12 (9-16)	49 (42-56)	> 1 mM	> 100	> 100
2	169	2.9 (2.2-3.8)	29 (27-32)	> 0.3 mM	> 100	20.5
3	202	0.25 (0.22-0.28)	110 (97-130)	0.27 mM	> 100	> 100
4[a]	210	7.2 (6.0-8.7)	190 (160-230)	> 1 mM	> 100	> 100
5	478	11 (9-13)	170 (140-190)	> 0.1 mM	> 100	77.8

[a] Values in brackets represent the 95% confidence interval in the K_i. The K_i was calculated according to the Cheng-Prusoff equation from a dose-response curve with three (technical) repeat measurements of enzyme activity at each concentration of compound.

[b] Compounds were tested to their solubility limit.

[c] Cell viability after 48h incubation with the compounds was assessed using Cell Titer Glo. See **Supplementary Figure 2** for complete dose response curves.

Table 2. *In vitro* activity of boronic acids 3.1-3.12 optimized for Gly137Asp *Lc*αE7 inhibition.

	K_i (nM)	
Compound	wildtype *Lc*αE7	Gly137Asp *Lc*αE7
3.1	0.70 (0.62-0.79)[a]	430 (380-500)
3.2	0.35 (0.31-0.40)	210 (180-230)
3.3	0.47 (0.36-0.59)	150 (130-170)
3.4	3.8 (2.9-4.9)	1000 (900-1200)
3.5	3.4 (2.6-4.5)	440 (350-550)
3.6	6 (5-9)	71 (60-85)
3.7	0.30 (0.26-0.35)	76 (69-85)
3.8	2.0 (1.7-2.4)	110 (100-120)
3.9	0.44 (0.39-0.50)	25 (22-27)
3.10	0.44 (0.33-0.56)	18 (16-20)
3.11	5.8 (4.1-8.0)	1000 (800-1200)
3.12	12 (9.2-15)	990 (870-1100)

[a] Values in brackets represent the 95% confidence interval in the K_i. The K_i was calculated according to the Cheng-Prusoff equation from a dose-response curve with three (technical) replicate measurements of enzyme activity at each concentration of compound.